The National IOR Centre of Norway

Methodological developments for ensemble-based optimization of EOR processes

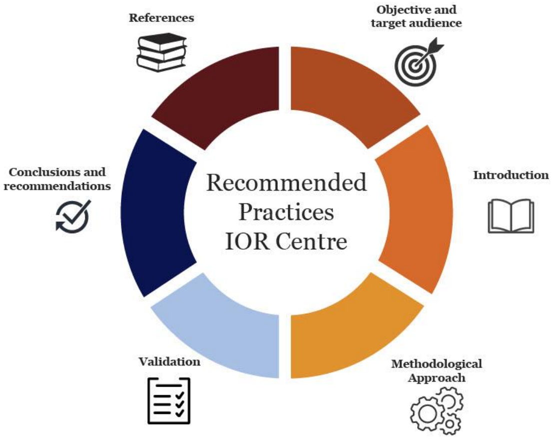

Yuqing Chang (NORCE)
Rolf J. Lorentzen (NORCE)
Geir Nævdal (NORCE)
30th November 2021

The National IOR Centre of Norway

Acknowledgement

The authors of recommended practices acknowledge the Research Council of Norway and the industry partners, ConocoPhillips Skandinavia AS, Aker BP ASA, Vår Energi AS, Equinor Energy AS, Neptune Energy Norge AS, Lundin Energy Norway AS, Halliburton AS, Schlumberger Norge AS, and Wintershall Dea Norge AS, of The National IOR Centre of Norway for support.


References
Objective and target audience
Conclusions and recommendations
Recommended Practices IOR Centre
Introduction
Validation
Methodological Approach

Contents

Objective and target audience

To plan an EOR campaign on a field we envision that an optimal injection scheme must be found. With the current advancement of ensemble-based methods for history matching, we foresee that the reservoir engineer might plan the production strategy based on an ensemble of history matched realizations of the reservoir model. By utilizing an ensemble of realizations of the reservoir model, the uncertainty in the reservoir description is accounted for. In this document we will present methodological development for ensemble-based optimization of EOR processes. For completeness, we also include some methodological development of ensemble-based optimization in general, and applications on optimization of reservoir drainage by waterflooding.

In the ensemble-based optimization, an ensemble-based approach is used to find an optimal strategy. There are a couple of advantages of this approach: (1) It works pretty efficiently for finding an optimal strategy over an ensemble of models; and (2) it can implemented non-intrusively with respect to the reservoir simulator (in our studies both ECLIPSE (ECLIPSE) and OPM Flow (OPM) has been used).

The document is in particular aimed at reservoir engineers and researchers that would get an introduction to ensemble-based optimization, including optimization of EOR processes on a reservoir scale. It would also give some results on comparing different EOR strategies, but these comparisons are of course case dependent and must be reassessed for other reservoirs. After reading the document, we hope that the reader can make a proper judgment if ensemble-based optimization is a suitable tool for finding optimal strategies for waterflooding or EOR processes for other reservoir models.

Introduction

Ensemble-based tools for production optimization has been developed over the last couple of decades, with a special focus on waterflooding. In our setting it will be important to expand this to include cases covering injection of smart water, CO_2 and polymer. Environmental constraints, including energy efficiency, should be added in the objective function. When considering implementation of any IOR or EOR method on a real field, it is of outermost importance to be able to demonstrate the potential, with as accurate as possible uncertainty quantification. Ensemble-based optimization has the potential to handle this as it can include all sources of uncertainties in the ensemble of reservoir models (also referred to as geological realizations).

In this document we will present ensemble-based optimization of waterflooding and EOR processes (CO_2, polymer and smart water). The optimization is performed to achieve a maximum net-present-value (NPV) for a given reservoir. The uncertainty in the reservoir description is included by providing an ensemble of reservoir models where important reservoir parameters (as porosity, permeability, etc.) varies. Economic input parameters includes oil price and cost of water injection and production as well as cost related to injection and production of EOR chemicals. In addition, a discount rate is included, but uncertainties in economical parameters are excluded.

The methodological development described in this document does not depend on any particular properties of the reservoir. However, for better illustration, two synthetic fields are chosen as demonstration cases. The two example cases are the OLYMPUS field designed by

TNO and the Reek field designed by Equinor. The OLYMPUS field is inspired and loosely based on Brent-type oil fields in the North Sea (Fonseca et al., 2018). The REEK field is a reservoir model developed in Equinor and originally used as an internal benchmark model for testing of different algorithms and workflows (Hanea et al., 2017).

The choice of these two fields for the demonstration of the methodology is based on a balance between including realistic features in the model and having models where a large number of simulations can be performed with modest computational resources. The computational time for a simulation of a waterflooding process on the OLYMPUS field is about 10 minutes. The computational time for actual field cases might be larger, but one of the strengths of ensemble-based optimization is that many of the required simulations can be run in parallel. Still, a judgment of the required computational load prior to performing the optimization will be important. For the methodological development that has been done as a part of the IOR center, it was preferable to work on cases with modest computational time, without sacrificing to much of realism. The OLYMPUS and REEK fields where considered as good choices in this respect. Moreover, these fields have both been used in other studies, making comparisons possible in some cases.

Methodological Approach

Recommended Optimization Workflow

A general workflow for ensemble-based optimization in the context of reservoir management is shown in Figure 1. Optimization algorithms play a key role for updating control variables in order to prepare for the input files for reservoir simulations. The evaluation of the objective function depends on output files from the simulator, which can be time consuming for large reservoirs, particularly for EOR processes. Therefore, the efficiency of the optimization algorithm is one of the concerns for this problem. In this aspect, ensemble-based optimization methods have attracted high interest in recent years. For the optimization tasks of the IOR Centre, we have investigated the use of ensemble-based optimization as this fits well with the task that using ensemble-based methods for history matching that has also been pursued within the IOR Centre.

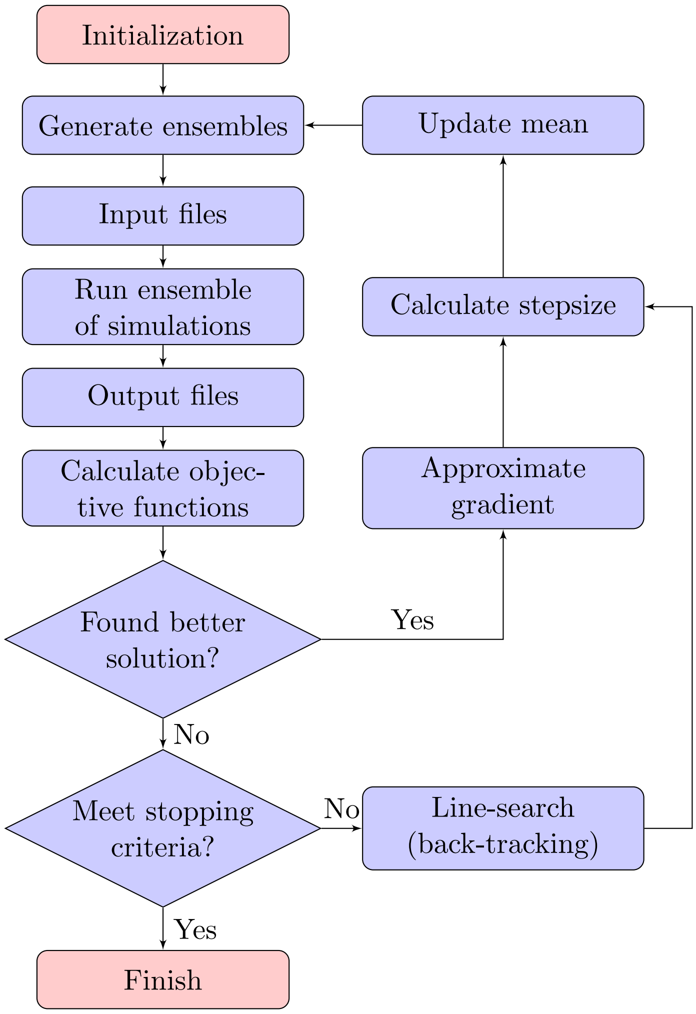

Figure 1: General optimization workflow for reservoir management.

There is a freedom in formulating the objective function. In the cases we have studied, it is formulated by calculating the net present value (NPV). The objective function should then account for the profit of the produced oil and costs of the injected and produced water. In addition, there comes the cost for injected and back-produced EOR gas or chemical.

Consider the net present value function $J(\mathbf{u},\boldsymbol{\theta})$ that depend on a set of control variables $\mathbf{u}$, and a state variable $\boldsymbol{\theta}$ that represents the geological realizations (reservoir models). In general, the same control strategy should run on an ensemble of reservoir models using the reservoir simulator (for example Eclipse or OPM Flow), and the expected NPV is calculated as the mean over the ensemble. The objective is to find $\mathbf{u}$ such that the expected value of J is maximized. This can be expressed mathematically as

$$J(\mathbf{u},\boldsymbol{\theta}) = \frac{1}{N_e}\sum_{j=1}^{N_e}\sum_{i=1}^{N_t}\Big[\frac{\big(r_o Q_{o,i}(\mathbf{u},\theta_j) + r_g Q_{g,i}(\mathbf{u},\theta_j)\big) - r_{w_I} Q_{w_I,i}(\mathbf{u},\theta_j) - r_{w_P} Q_{w_P,i}(\mathbf{u},\theta_j) - R_{i,j}}{(1+d_\tau)^{\frac{t_i}{\tau}}}\Big] \tag{1}$$

where the index j represents the ensemble member, the index i the time step, N_e is the number of ensemble members and N_t is the number of time steps. d_τ is the discount rate for a period of time τ (days); t_i is the sum total time (days) from the start of production up to the ith time steps; Δt_i is the period of time (days) between the time steps t_i and t_{i-1}; $Q_{o,i}$ and $Q_{g,i}$ are the total amount of oil and gas production over the time interval Δt_i; $Q_{w_I,i}$ and $Q_{w_P,i}$ are the total amount of water injection and production in time Δt_i; r_o, r_{w_I}, r_{w_P}, and r_g represent the price of produced oil, cost of water injection and production, and the price of gas production respectively. The term $R_{i,j}$ represents the cost of injection and back producing of a EOR chemical/gas for time step i and ensemble member j, and it might have the form

$$R_{i,j} = r_I Q_{I,i}(\mathbf{u}, \theta_j) + r_P Q_{P,i}(\mathbf{u}, \theta_j)$$

where $Q_{I,i}$ and $Q_{P,i}$ are the total amount of EOR chemical injection and production over the time interval Δt_i respectively; and r_I and r_P are the costs of injection and production of the EOR chemical, respectively. For all the quantities in the above equations, appropriate units must be chosen. (In the case of optimization of a plain waterflooding case $R_{i,j}$ can be omitted.)

The optimization problem is now to find the optimal vector $\mathbf{u}$ maximizing $J(\mathbf{u}, \boldsymbol{\theta})$ over all admissible vectors $\mathbf{u}$. The length of the vector $\mathbf{u}$ depends on the formulation of the optimization problem. The control vector $\mathbf{u}$ will depend on the steering of the wells, how frequent the strategy can be changed, and so forth. For example, it can be set that the injection and production rates for each well can be changed every three months over the optimization window (assuming a pure waterflooding case). Typically, there will be some bound constraints on the variables, u_i, for instance representing the fact that a production rate must be non-zero and below some upper bound for the allowable production from that well. In addition, we will have “output constraints” which is very commonly used during petroleum production. These are non-linear constraints that represent operational limits and they are usually evaluated using the reservoir simulator. A typical example is pressure limits for injectors or producers in a model where the wells are operated using flow rate targets (given by the control variables).

Ensemble-based Optimization (EnOpt)

The EnOpt method and its variations have been widely implemented in various application. Here, we will briefly introduce the concept and some key formulas for this algorithm. Some references for more details are Chen et al. (2009), Fonseca et al. (2017).

A conceptual diagram of EnOpt can be found in Figure 2. Assume we need to find an optimal solution within a feasible region that optimize the objective function shown in Equation (1). We first set a starting point $\mathbf{u}_0$, and decide for an initial covariance matrix to use for the sampling of data points. For a general step (including the first), the current best solution is given as $\mathbf{u}_k$ which is set as the mean in a multinormal distribution. We generate an ensemble of data points around the mean with a predefined covariance matrix. The data points are then evaluated to get objective function values in order to approximate the gradient $\mathbf{G}_k$. If the objective function is improved, we update the mean to $\mathbf{u}_{k+1}$, otherwise, we do a line-search to seek for other possible solutions. This process is repeated iteratively until the algorithm converge. The optimal solution $\mathbf{u}^*$ is found when the algorithm is finished.

Originally the EnOpt algorithm was proposed as an approximation to the pre-conditioned steepest ascend method

$$\mathbf{u}_{k+1} = \mathbf{u}_k + \beta_k \frac{\mathbf{C}_{\mathbf{u}}^k \mathbf{G}_k^\top}{||\mathbf{C}_{\mathbf{u}}^k \mathbf{G}_k^\top||_\infty}, \tag{2}$$

where k = 0,1,2,... is the index for optimization iteration; β_k is step size obtained by simple auxiliary search method (Nocedal and Wright, 2006), $\mathbf{G}_k$ is the approximate gradient vector of the objective function in Equation (1) with respect to $\mathbf{u}_k$, $\mathbf{C}_{\mathbf{u}}^k$ is the user-defined covariance matrix of the components of $\mathbf{u}_k$, and $||.||_\infty$ is the infinite norm.

The combination $\mathbf{C}_{\mathbf{u}}^k \mathbf{G}_k^\top$ can be approximated using the simple cross-covariance between $\mathbf{u}_k$ and the objective function $J(\mathbf{u}_k, \boldsymbol{\theta})$ (see the details in (Chen et al., 2009)). In the presence of geological uncertainty, Fonseca et al. (2017) implemented an improved version of the gradient approximation which has the form

$$\mathbf{C}_{\mathbf{u}}^k \mathbf{G}_k^\top \approx \frac{1}{N-1} \sum_{j=1}^{N} (\mathbf{u}_{k,j} - \mathbf{u}_k)\big(J(\mathbf{u}_{k,j}, \theta_j) - J(\mathbf{u}_k, \theta_j)\big). \tag{3}$$

(Here $J(\mathbf{u}, \theta_j)$ denotes evaluating the objective function using control strategy $\mathbf{u}$ for the reservoir simulation model θ_j, (i.e., a single ensemble member j is used in (1) whereas $J(\mathbf{u}, \boldsymbol{\theta})$ denotes evaluating the full objective function (1) which requires evaluating all the ensemble members for the control $\mathbf{u}$.

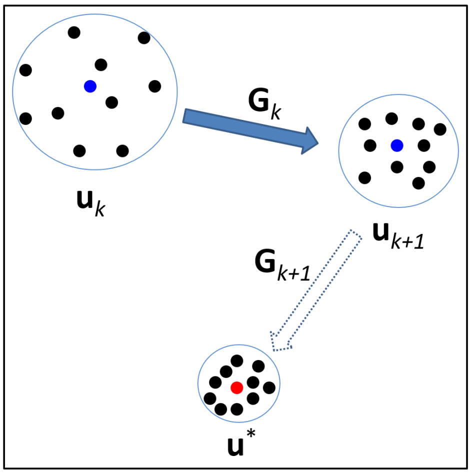

Figure 2: A conceptual diagram of the EnOpt algorithm.

The optimization process continues until the updating scheme converges. In this study, the scheme converges when the following criteria is sufficiently satisfied:

$$\frac{|J(\mathbf{u}_{k+1}, \boldsymbol{\theta}) - J(\mathbf{u}_k, \boldsymbol{\theta})|}{|J(\mathbf{u}_k, \boldsymbol{\theta})|} \leq \epsilon, \tag{4}$$

where ϵ is a given tolerance.

For the initialization and update of covariance matrix $\mathbf{C}_{\mathbf{u}}^k$, we refer to the work of Stordal et al. (2016).

Constrained Optimization with Exterior Penalty Function (EPF)

In reservoir management, the liquid injection and production process yield to certain constraints. Therefore, the optimization of the objective function is subject to a well-defined set of constraints on the designed control variables (such as the water rate of each injecting well at each control time step, etc.). In this section, we present a general constrained optimization (maximization) problem, often encountered in science and engineering. The work is based on the paper by Oguntola and Lorentzen (2021a). In that paper the methodology is demonstrated for traditional water-flooding, and the results are not repeated here, but we include the principles for solving constrained optimization problems.

If we convert the maximization problem to a minimization problem, $f(\mathbf{u}) = -J(\mathbf{u})$, then the general N_u-dimensional constrained optimization problem is written as

$$\min_{\mathbf{u}\in\mathbb{R}^{N_u}} \quad f(\mathbf{u}) \tag{5}$$

$$\text{subject to:} \quad g_i(\mathbf{u}) \geq 0, \quad \forall i \in \mathrm{I} \tag{6}$$

$$h_j(\mathbf{u}) = 0, \quad \forall j \in \mathrm{E}, \tag{7}$$

where g_i and h_j are the underlying constraint functions (from $\mathbb{R}^{N_u}$ into $\mathbb{R}$ respectively), I and E are the indexing sets for the inequality and equality constraints respectively. Any bound constraints that applies can be rewritten in the form (6).

Suppose that a given constrained optimization problem is in the form of Equations (5) - (7). Let $\mathcal{D} \subset \mathbb{R}^{N_u}$ be the domain of feasible solutions. Hence, $\mathbb{R}^{N_u}\backslash\mathcal{D}$ is the set of infeasible points. To solve the problem, first, we transform it into a sequence of unconstrained subproblems using the exterior quadratic PF method. In each subproblem, $P_k,\ k = 1, 2, ...$, is a penalty function defined as follows;

$$P_k(\mathbf{u}, r_k) = f(\mathbf{u}) + r_k\Big(\sum_{i\in\mathrm{I}}(\min\{g_i(\mathbf{u}), 0\})^2 + \sum_{j\in\mathrm{E}}|h_j(\mathbf{u})|^2\Big). \tag{8}$$

It can be shown that the following sequence of unconstrained subproblems converges to a feasible solution:

$$\min_{\mathbf{u}\in\mathbb{R}^{N_u}} \quad P_k(\mathbf{u}, r_k), \quad \forall k = 1, 2, ..., \tag{9}$$

where r_k is an increasing sequence of positive penalty parameters. We use a simple relation for the penalty parameters given by $r_{k+1} = cr_k, \quad k = 1, 2, ...$, where $c \geq 1$ and the first term, $r_1 > 0$, are carefully selected constants.

Validation

The developed approach has been validated through testing on three models with increasing complexity. The first example is a classic synthetic 2D reservoir with a 5-spot configuration of the wells, with an injector in the center and one producer in each of the four corners. The second model used for the verification is the REEK model, a synthetic model developed by Equinor. Finally, we present some result on the synthetic OLYMPUS field, designed by TNO, inspired by a Brent like reservoir.

EOR methods for a 5-spot case

In this section the workflow is validated using EnOpt to solve the optimization problem (1) using polymer, CO_2, and smart-water (brine) EOR methods. We used optimization results to quantify the values (with traditional water flooding as a reference point) and rank of EOR methods. The value quantification of the EOR methods involves evaluating the economic benefits (in terms of oil and water productions and expected NPV) of the EOR optimal solutions compared to that of water flooding.

We consider a synthetic 2D 5Spot oil field with a single ($N_e = 1$) reservoir model. It has three-phase flow (including oil, water and gas). There are four producers and one injection well arranged in a five-spot pattern as depicted in Figure 3. The model is uniformly discretized into 50 × 50 grid cells, with $\Delta x = \Delta y = 100$ m. It has approximately 30% porosity with heterogeneous permeability map. The initial reservoir pressure is 200 bar. The original oil in place (OOIP) is 4.983×10^6 sm^3. Fluid properties is close to that of a light oil reservoir.

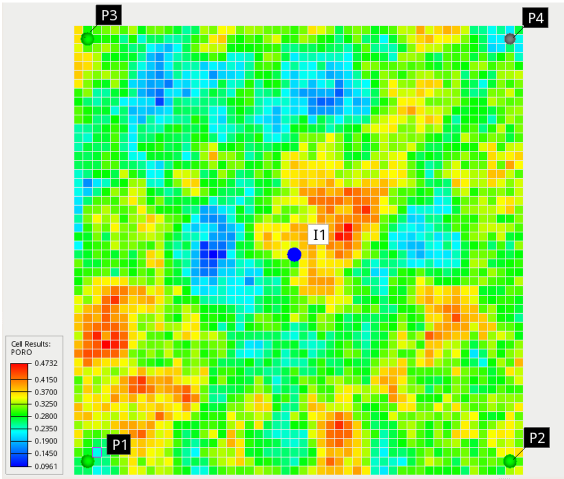

Figure 3: Porosity distribution of the five-spot field

The optimized NPV and total field oil production is shown on Figure 4. For this study, CO_2 injection achieve the highest NPV and total oil production. All EOR methods outperform traditional water flooding. For more details we refer to Oguntola and Lorentzen (2021b).

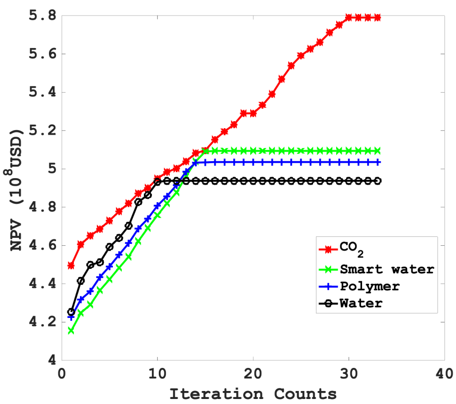

(a) NPV variation

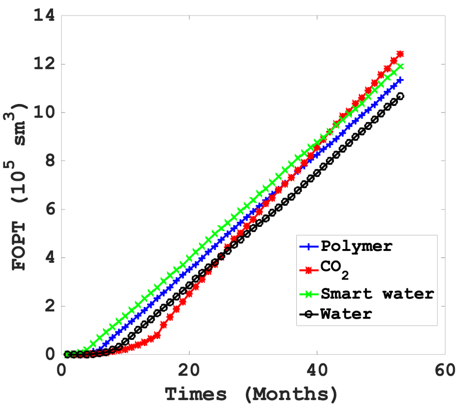

(b) Field Oil Production Total

Figure 4: (a) Comparison of the change in NPV with iteration for the EOR-methods and water flooding for the 5Spot field. (b) Comparison of the field oil production total (FOPT) from optimal solutions for the EOR methods and water flooding for the 5Spot field.

EOR methods for the Reek field

In this case, we consider a more complex 3D optimization problem with geological uncertainties and examine impact on EOR effects. The tests are performed on the synthetic Reek field designed by Equinor. The reservoir has three-phase flow (including oil, water, and gas). It is defined on an irregular grid system of dimensions $40 \times 64 \times 14$ partitioned into 35840 grid cells with different sizes. The reservoir has three zones (UpperReek, MidReek, and LowerReek) with six faults and different porosity and permeability. The model is equipped with five producing and three injecting wells (see Figure 5). All producers and one injector are spatially positioned throughout the oil-containing region, while the remaining two injectors are in the water saturated zones on the accord of engineering intuition. Like in the 5-spot reservoir, fluid properties are similar to that of a light oil reservoir. Moreover, we consider and quantify uncertain properties such as facies, porosity, permeability, oil-water contacts, and transmissibility across five faults (out of the six). Fifty geological realizations ($N_e = 50$) are used to account for these uncertainties in the reservoir. Although there are 35840 grid cells, not all of them are active. The number of active cells varies with geology. On average, the original oil in place (OOIP) is 4.831×10^7 sm^3.

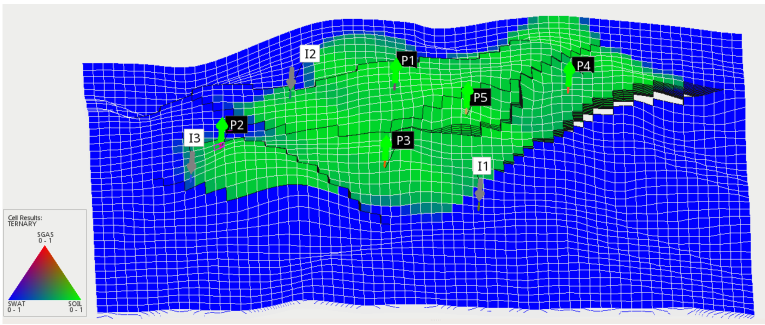

Figure 5: The initial saturation map for oil, water and gas of the Reek field.

The optimized NPV for the different EOR methods are shown on Figure 6a. Also in this case the CO_2 method achieve the best NPV. Figures 6b and 6c show the total oil production and total water production, for the 50 geo-models. From these plots we see that CO_2 has generally higher oil production and lower water production, compared to the other methods. Polymer injection generates highest water production. The results are sensitive to the cost of the injected CO_2 or chemicals. The cost translate to solving optimization problems with different objective functions, and it is paramount to use values that reflect the current market and tax level for practical application. For more details we refer to Oguntola and Lorentzen (2021b).

EOR using waterflooding and polymer on the Olympus case

The optimization workflow using EnOpt was validated on the benchmark case OLYMPUS field (TNO, 2017). The OLYMPUS field (Figure 7) is a synthetic reservoir model prepared by TNO (TNO) for an exercise in field development optimization (Chang et al., 2019). Here, we consider the well control problem from a different perspective by using well economic limits (WECON) and injection pressures as parameters to optimize the objective function - the Net Present Value (NPV). The WECON is quantified by the water cut values in this work.

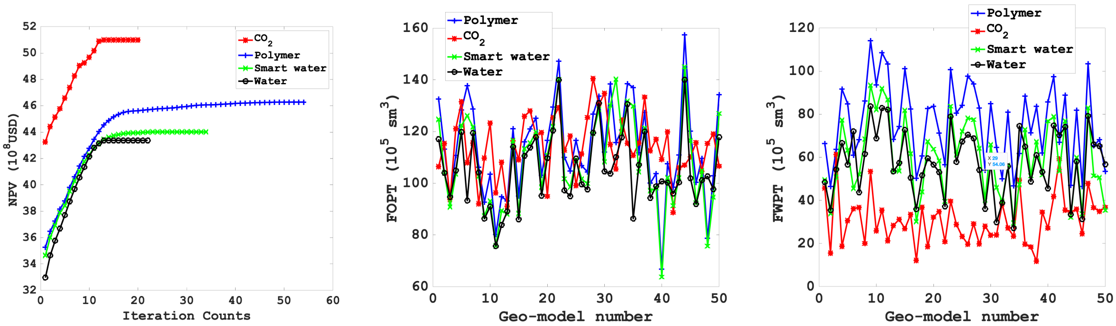

(a) NPV variation (b) FOPT (c) FWPT

Figure 6: (a) Comparison of the change in NPV with iteration for the EOR-methods and water flooding for the Reek field. (b) Comparison of the field oil production total (FOPT) from optimal solutions for the EOR methods and water flooding for the Reek field. (c) Comparison of the field water production total (FWPT) from optimal solutions for the EOR methods and water flooding for the Reek field.

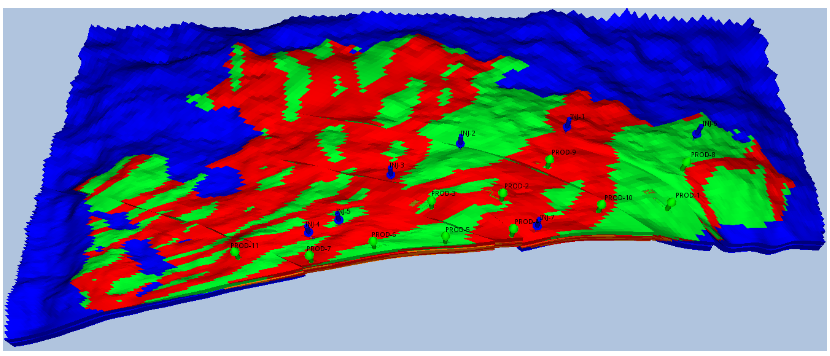

Figure 7: OLYMPUS case with reference wells. The field shows oil saturation for the first model realization. Red, green, and blue represent approximately 0.92, 0.43, and 0, respectively.

Because of the stochastic behavior of EnOpt methods, multiple starting points and repeating experiments with different random seeds are recommended. Same as in this study, we had different experiments and the results of the experiment which gives the best NPV is shown in Figure 8. Figure 8a shows that the starting value of WECON at 0.88 is suboptimal, and some wells become uneconomical earlier than when the water cut reaches 0.88, while other wells are eligible to produce at a higher water cut. In Figure 8b, the red stars show the trial steps that are not successful during the optimization. In this case, the back-tracking step size failed to improve the objective function for 3 times and the covariance adjustment failed twice before the EnOpt algorithm stops. The optimal WECON values of each producer are listed in Table 1.

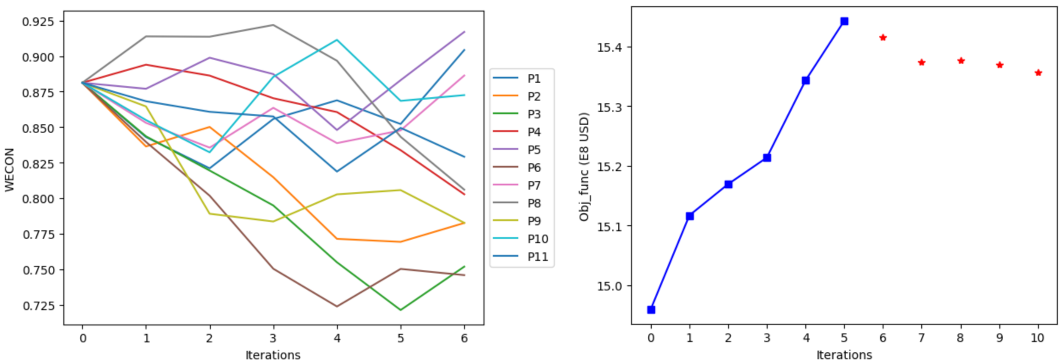

(a) WECON (b) Objective function

Figure 8: Optimization results of the best run. Evolution of the control variables (WECON), the objective function, the step size and the ensemble perturbation covariance during each iteration. The red stars in the objective function plot represents the failed trial steps during the optimization.

Table 1: Optimal values of WECON from the best run.

	P1	P2	P3	P4	P5	P6	P7	P8	P9	P10	P11
Optimal Values	0.90	0.78	0.75	0.80	0.92	0.74	0.89	0.80	0.78	0.87	0.83

Using the optimal solution of injector BHP of Chang et al. (2019) as one of the starting points, we had several extra experiments and the highest NPV achieved is $\$15.74 \times 10^8$. The total number of simulations required to reach this optimal solution was 2350, which is ten times more efficient compared to the computational cost of Silva et al. (2019), which achieved a slightly higher NPV with ten times more simulations. This shows the efficiency of the EnOpt method. Because EnOpt requires relatively small number of simulations, it gives us the opportunity to repeat the experiments multiple times, which may find better results than what we can obtain with only one run of the optimization workflow.

The ensemble-based method for EOR is validated using polymer for the OLYMPUS field (see also Oguntola and Lorentzen (2020)). At the time of this experiment, some EOR functionalities in the OPM Flow simulator was not fully developed for CO2 and smart-water EOR processes. The objective function of the optimization problem is the NPV given by Equation 1. In the study we assume that there is polymer desorption with no degradation. We simulate reservoir fluid flow using the Open Porous Media (OPM) Flow simulator (OPM). We obtain the optimal well controls for polymer flooding that maximize the objective function, and compare the result with optimized conventional continuous water flooding. The benefit is not only increased oil recovery, but also reduced cost and environmental impact due to reduced water and polymer injection and production. The results for polymer flooding (PF) and continuous water flooding (CWF) is shown on Figure 9.

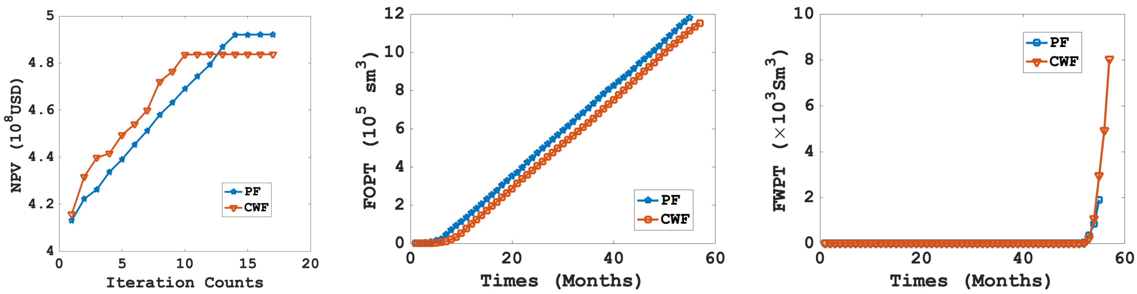

Figure 9: Comparison of the change in NPV with iteration for CWF and PF (left). Comparison of the field oil production total (FOPT) from optimized CWF and PF (middle). Comparison of the field water cut (FWPT) from optimized CWF and PF (right).

Conclusions and recommendations

Ensemble-based optimization has been demonstrated as a useful tool for optimization of waterflooding processes, and with the recent works (Oguntola and Lorentzen, 2021b, 2020) also for optimization of EOR processes. Although the field cases used in the presented studies are synthetic, one can easily apply the methodology to real fields as well. For more complex models, some considerations about the computational time might be required before a decision on running ensemble-based optimization is done. The computational performance will depend on a number of factors, including the size of the ensemble of reservoir models used to account for the uncertainty. The computational time will decrease substantially if the reservoir simulations can be run in parallel. An issue to consider in the formulation of the optimization problem is the number of optimization variables. It might be easier to obtain good estimates of the gradients with fewer variables. It is still a topic for further research to improve the methodology for ensemble-based optimization.

Ensemble-based optimization is easily adapted both with respect to the choice of reservoir simulator (in our studies ECLIPSE (ECLIPSE) and OPM Flow (OPM) has been used) and the formulation of the optimization problem. In our case, a wrapper has been constructed that produces input files depending on the current setting of the optimization variables and reads the required output from the simulations to calculate the objective function. There is no need for doing any internal coding in the simulator, making it easier to get started with doing the optimization.

The primary purpose of the described optimization algorithm is to improve the economic impact of the reservoir by finding good strategies for the production. The environmental impact is in our studies accounted for by including cost terms in the objective function for produced and injected water and EOR chemicals. Some adaptions might be needed to handle a case when there is, say, a limit on the allowed amount of back produced polymer.

It will obviously increase the impact of the present work if the methodology is included in a more streamlined workflow, as for instance in software developed for ensemble-based history matching or fast model updating. Since the developed methodology for optimization of EOR processes is rather new, it is to our knowledge, not yet tested at any field on NCS.

References

Y. Chang, R. J. Lorentzen, G. Nævdal, and T. Feng. OLYMPUS optimization under geological uncertainty. *Computational Geosciences*, 24:2027–2042, 2019. doi:10.1007/s10596-019-09892-x.

Y. Chen, D. S. Oliver, and D. Zhang. Efficient ensemble-based closed-loop production optimization. *SPE Journal*, 14(04):634–645, 2009.

ECLIPSE. Eclipse™. `https://www.software.slb.com/products/eclipse`. Accessed: 2021-09-22.

R. M. Fonseca, B. Chen, J. D. Jansen, and A. Reynolds. A stochastic simplex approximate gradient (StoSAG) for optimization under uncertainty. *International Journal for Numerical Methods in Engineering*, 109(13):1756–1776, 2017.

R. M. Fonseca, E. D. Rossa, A. A. Emerick, R. G. Hanea, and J. D. Jansen. Overview of the olympus field development optimization challenge. In *ECMOR XVI 2018 – 16 th European Conference on the Mathematics of Oil Recovery*. EAGE, September 3-6 2018.

R. Hanea, P. Casanova, F. H. Wilschut, and R. Fonseca. Well trajectory optimization constrained to structural uncertainties. In *SPE Reservoir Simulation Conference*. Society of Petroleum Engineers, 2017.

J. Nocedal and S. Wright. *Numerical optimization*. Springer Science & Business Media, 2006.

M. Oguntola and R. Lorentzen. On the robust value quantification of polymer EOR injection strategies for better decision making. In *ECMOR XVII*, volume 2020. European Association of Geoscientists & Engineers, 2020.

M. B. Oguntola and R. J. Lorentzen. Ensemble-based constrained optimization using an exterior penalty method. *Journal of Petroleum Science and Engineering*, 207:109165, 2021a. ISSN 0920-4105. doi:10.1016/j.petrol.2021.109165.

M. B. Oguntola and R. J. Lorentzen. Robust value quantification of enhanced oil recovery methods using ensemble-based optimization. Submitted to "SPE Reservoir Evaluation & Engineering", 2021b.

OPM. Open porus media. `https://opm-project.org/`. Accessed: 2021-09-22.

V. L. S. Silva, M. A. Cardoso, D. F. B. Oliveira, and R. J. de Moraes. Stochastic optimization strategies applied to the OLYMPUS benchmark. *Computational Geosciences*, Oct 2019. doi:10.1007/s10596-019-09854-3.

A. Stordal, Y. Chang, R. Hanea, and T. Ek. Ensemble based optimization using importance sampling and gaussian mixtures. In *ECMOR XV-15th European conference on the mathematics of oil recovery*, 2016.

TNO. `https://www.tno.nl/en/`. Accessed: 2021-09-29.

TNO. OLYMPUS optimization challenge. `http://www.isapp2.com/optimization-challenge/problem-statement.html`, 2017. Accessed: 2021-09-22.